Environmental Chemistry and Ecotoxicology 6 (2024) 380–389

Contents lists available at ScienceDirect

Environmental Chemistry and Ecotoxicology

journal homepage: www.keaipublishing.com/en/journals/environmental-chemistry-and-ecotoxicology/

Tire-wear particle leachate at environmentally relevant concentrations exert a hepatotoxic impact on the black-spotted frog by disrupting the gut–liver axis

Zhiquan Liu [a,b], Hongmei Yang [b], Yinan Zhang [b], Yongjian Shao [b], Shuangqing Hu [a], Hangjun Zhang [b], Genxiang Shen [a,*]

[a] State environmental protection key laboratory of environmental health impact assessment of emerging contaminants, Shanghai academy of environment sciences, Shanghai 200233, PR China
[b] School of engineering, Hangzhou Normal University, Hangzhou 311121, PR China

ARTICLE INFO

Keywords:
Tire-Wear Particles
Hepatotoxicity
Gut–liver axis
Oxidative damage
Lipopolysaccharide

ABSTRACT

As global surface water pollutants, tire-wear particles (TWPs) are increasingly concerning, with TWP leachate hepatotoxicity poorly understood. In this study, based on environmental TWP concentrations, TWP leachate exposure (0, 0.0005, 0.005, 0.05, and 0.5 mg/mL) in black-spotted frogs was investigated over a 21 day period. TWP leachates at realistic environmental levels disturbed intestinal microbiome homeostasis, which manifested as decreased and increased *Chloroflexi* and *Proteobacteria* abundance, respectively, and elevated lipopolysaccharide (LPS) levels in plasma. Also, the content of lipopolysaccharide-binding protein, the binding site of LPS, was increased, and downstream LPS immune pathways, such as toll-like receptor 4 (TLR4)-nuclear factor (NF)-κB (TLR4/NF-κB) signaling, were activated. Subsequently, inflammation reactions, oxidative damage, and histopathology were affected in liver samples. These results shed new light on the potential mechanisms underpinning TWP leachate-associated liver injury via the gut–liver axis, and contribute to a better understanding of emerging TWP ecotoxicology.

1. Introduction

Tire-wear particles (TWPs) are primarily produced via friction between tires and road surfaces. Critically, approximately 6.1 million tons of TWPs are released into the environment each year [1]. As global car production is expected to increase to 90 million units in 2024, TWP levels will likely increase. TWPs are considered a principal microplastic [2–4] and account for approximately 42% of the microplastic pollution in aquatic environments [5]. As a typical emerging pollutant, TWPs are widely detected in global surface waters. TWP concentrations occur at 0.09–6.3 mg/L [6] in surface waters, 0.3–155 g/kg [7] in sediments, and 0.5–563 mg/L in snow, surface runoff, and river waters [8,9].

The additive chemicals in TWPs do not covalently bind to polymers, and may be released into liquids at any stage of the plastic life cycle [10]. Therefore, TWPs may release chemicals into aquatic environments, which may account for TWP toxicology [11,12]. Therefore, the adverse effects of TWP leachates on organisms in the environment must be determined. The TWP leachates could cause mortality to the zooplankton, and trigger oxidative stress in crab and algal [13–15]. Since TWP leachates are considered global contaminants of concern, several adverse effects have been identified, e.g., liver toxicity [14,16]. When affected by environmental pollutants, the liver is targeted by various drugs and pollutants and is very prone to damage [17]. Inflammatory liver responses are accompanied by oxidative stress, which is a series of adaptive responses caused by an imbalance between reactive oxygen species (ROS) and the antioxidant system [18]. Environmental pollutant exposure can also induce hepatocytes to produce ROS, induce intracellular oxidative stress, and rapidly trigger hepatocyte injury. TWPs are reported to induce oxidative stress in earthworms [19]; however, TWP mechanisms remain poorly understood.

Increasing evidence links the gut microbiota to the liver, namely the gut–liver axis [20,21]. Disrupted intestinal microbial flora homeostasis may cause liver dysfunction via bidirectional gut–liver communications, the majority of which are mediated by immune factors or metabolites produced by intestinal microbial flora, e.g., lipopolysaccharide (LPS). This flora is particularly susceptible to exogenous stressors, including

* Corresponding author.
E-mail address: shengx@saes.sh.cn (G. Shen).

https://doi.org/10.1016/j.enceco.2024.08.004
Received 10 July 2024; Received in revised form 12 August 2024; Accepted 13 August 2024
Available online 14 August 2024

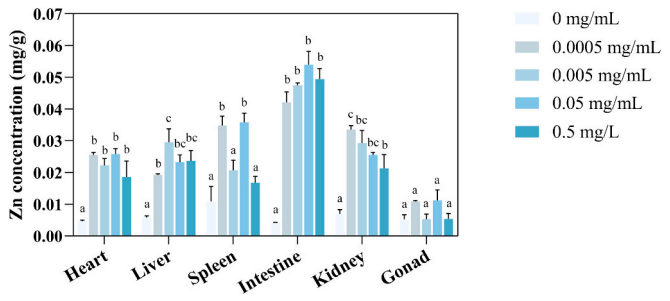

Fig. 1. Zinc bioconcentrations in heart, liver, spleen, intestine, kidney, and gonad samples from black-spotted frogs after TWP leachate exposure for 21 days. Data are expressed as the mean ± standard deviation. Different letters denote significant differences between treatments.

environmental contaminants, which are potent disruptors of gut microbiota homeostasis [22–24]. However, it remains unclear if TWP leachate exposure modifies gut microbiota community structures and if microbial disorders mediate liver toxicology induced by this exposure.

Amphibians are indicator species that monitor ecosystem health and have pivotal roles in aquatic and terrestrial ecosystems [25]. As key links in such ecosystems, declining amphibian populations pose serious threats to the biodiversity of their predators, e.g., snakes, and may also increase harmful insect numbers, which impact on grain production [26]. Currently, environmental pollution has threatened approximately 19% of amphibian populations worldwide [27]. The black-spotted frog (*Pelophylax nigromaculatus*) is a native amphibian species in China, with highly permeable skin [28] and highly susceptible to pollutants. Previous studies have confirmed that *P. nigromaculatus* is a suitable organism for toxicology research [29–32].

To examine TWP leachates in ecosystems, we investigated their hepatotoxicity in black-spotted frogs using histological and liver injury indicator analyses (e.g. alanine aminotransferase (ALT) and aspartate transaminase (AST)). Transcriptomic analyses were also performed. Also, to examine the gut–liver axis and its potential involvement in hepatotoxicity, the intestinal microbiota was analyzed using *16S rRNA* sequencing, from which intestinal microbial diversity and community composition were both analyzed. We also examined downstream pro-inflammatory cytokine expression, including interleukin (IL)-6, IL-1β, tumor necrosis factor (TNF)-α, and oxidative stress-related content and enzymes, including O^{2-}, hydrogen peroxide (H_2O_2), malondialdehyde (MDA), superoxide dismutase (SOD), glutathione-S-transferase (GST), and glutathione peroxidase (GPX). Our results highlight gut–liver axis mechanisms induced by TWP leachates at environmental concentrations during hepatotoxicity in amphibians.

2. Material and methods

2.1. TWPs and leachate preparation

An old tire (Bridgestone Tires 235/50R18 97 V H/P SPORT MOE) was purchased from a car repair company, crushed into approximate 300 mm pieces at a tire recycling unit, and further crushed into smaller particles using a fine crusher (**Fig. S1**). The tires were first treated with liquid nitrogen, and then ground using grinder to make TWP. A 500 μm mesh was used to remove larger tire particles. The main TWP components, including organics, carbon black, metals, and polymers, were quantified by thermogravimetric analysis (TGA, **Supporting Information Text S1**) and X-ray fluorescence spectrometry (XRF, **Supporting Information Text S2**). TGA showed that the predominant substances in tire mixtures were organic rubber (70%), with the remainder including carbon black (16%), zinc (Zn) oxide, and other fillers (14%) (**Fig. S2**). A variety of metals were detected by XRF and confirmed as Zn, Si, S, Ca, Fe, K, Ni, P, Ta, AI, Br, Ti, Cu, and Cr, with Zn (57.7%) accounting for the highest proportion (**Fig. S3**).

Subsequence, 12 mg of TWPs were added to 300 mL of a pure aqueous solution in a clean Erlenmeyer flask, and extracted by shaking at 200 rpm for 1 week at room temperature. Finally, to eliminate debris, suspended solids, or microbial contaminants, leachates were passed through 0.22 μm cellulose acetate filters (Corning, New York, USA) [33] (**Fig. S1**). The finally leachates were used for subsequence exposure experiments.

2.2. Experimental design

In this study, *Pelophylax nigromaculatus* (black-spotted frog - test organism) was purchased from Hubei Jingrong Agricultural Products Professional Cooperative (Hubei, China). Frogs were housed in a laboratory glass tank (60 cm × 40 cm × 35 cm) and provided with 12 h of

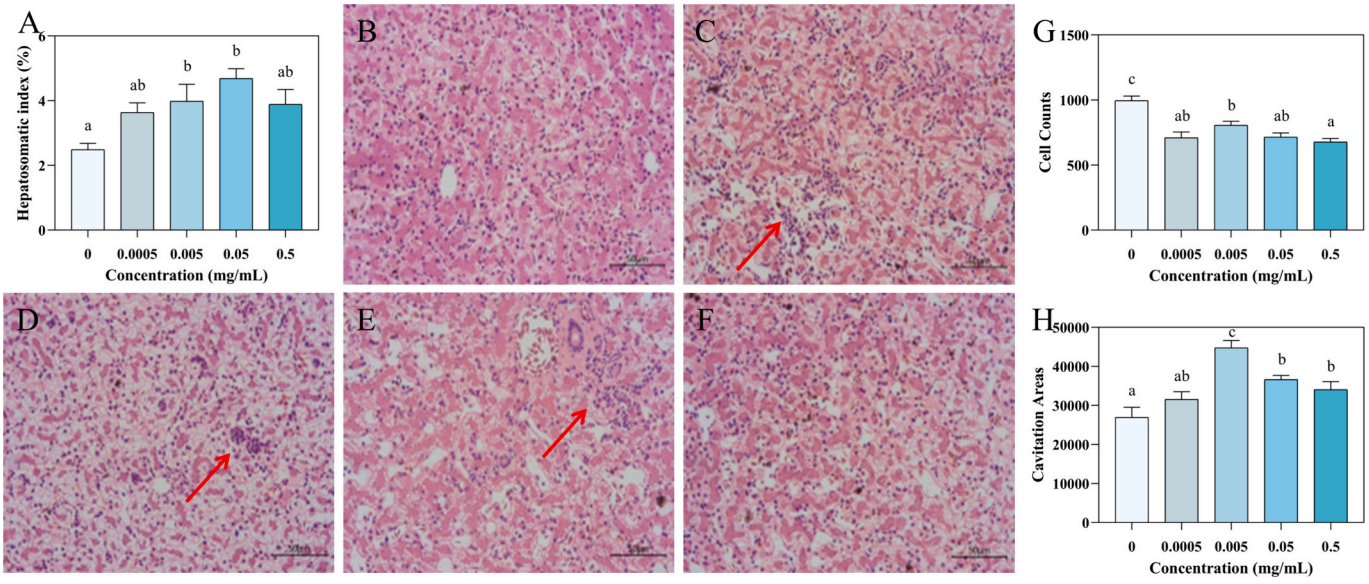

Fig. 2. Liver histopathology and inflammatory factor levels in black-spotted frogs. (A) Liver volume ratios in male frogs; (B–F) Hematoxylin-eosin staining of liver sections after TWP leachate exposure; (G) Nuclei numbers in liver tissues; (H) Vacuolar areas in liver tissue sections. Different letters denote significant differences between treatments.

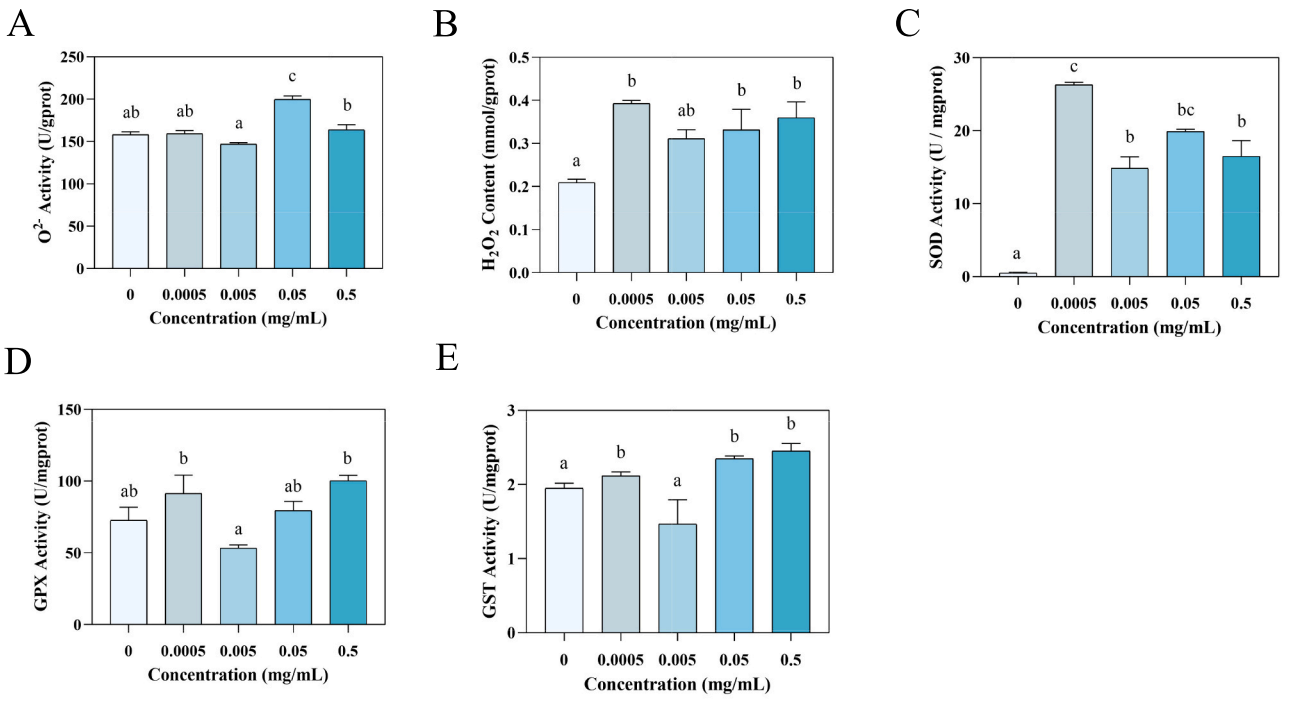

Fig. 3. Superoxide anion (A; $n = 3$), hydrogen peroxide (B; n = 3), and superoxide dismutase (C; n = 3) activities, and glutathione peroxidase (D; n = 3) and glutathione S-transferase (E; n = 3) content in frog livers after exposure (21 days) to controls and TWP leachates (0.0005, 0.005, 0.05, and 0.5 mg/mL). Different superscripts indicate significant intergroup differences at $p < 0.05$.

natural and 12 h of dark periodic light [31] for 7 d for acclimatization. Healthy adult male frogs of similar weight (approximately 30 g) were selected for exposure experiments. Frogs were divided into five treatment groups, corresponding to 0, 0.0005, 0.005, 0.05, and 0.5 mg/mL solutions (temperature = 20 ± 1 °C; pH = 6.5 ± 0.5; and dissolved oxygen content = 7 ± 1 mg/L). Exposure concentrations were based on environmental TWP concentrations in frog habitats (0.5–563 mg/L) [34].

After 21 days of exposure, frogs were humanely sacrificed by cerebrospinal cord puncture, livers and intestinal tissues collected, adhesions removed, tissues weighed (on ice), and finally tissues washed in normal saline. Part of the liver was fixed in 4% paraformaldehyde for histomorphological analyses, while the remainder was placed in centrifuge tubes, snap-frozen in liquid nitrogen, and stored at −80 °C. Blood was collected via cardiac puncture into 5 mL vacuum blood collection tubes, and centrifuged at 4 °C and 4000 rpm for 10 min to separate serum, which was stored at −80 °C. To reduce individual differences and highlight biologically significant changes, three samples were combined for analyses. Animal experiment procedures followed guidelines established by the Association for the Science of Laboratory Animals and were approved by the Animal Ethics and Welfare Committee of Hangzhou Normal University.

2.3. Zn content assessments

As a TWP leachate marker, the trace metal Zn has been identified in exposure solutions and the frog tissues, including liver, kidney, spleen, heart, intestine, and gonads. More information could be found in **Supporting Information Text S3 and S4.**

2.4. Liver tissue morphology assessments

Hematoxylin-eosin staining was used to analyze liver tissues after 21 days of TWP leachate exposure. Liver tissues ($n = 3$ replicates) were stored overnight at 4 °C in 10% neutral formalin fixative, after which they were dehydrated in an ethanol concentration gradient and embedded in paraffin. Fresh liver tissue was placed in neutral formalin and fixed overnight, followed by an ethanol concentration gradient, then fully saturated in xylene, and transferred and immersed in wax. Tissues were continuously cut into 4 μm sections, stained in hematoxylin-eosin, and finally sealed after the xylene became transparent [35]. Histopathological evaluations were performed under light microscopy (Nikon, 200× magnification, Nikon, Japan) and quantitative analyses performed in Image J.

2.5. Biochemical measurements

Random livers from three frogs in the same concentration group were weighed and combined, after which 0.65% saline was added in a mass (g): volume (mL) ratio = 1:9. Samples were homogenized using three grinding beads in a tissue grinder (JXFSTPRP-24 L, Jingxin, China), centrifuged at 2500 rpm for 10 min at 4 °C, and supernatants removed and analyzed. AST (C010–2-1), ALT (C009–2-1), GST (A004–1-1), GPX (A005–1-2), SOD (A001–3-2), MDA (A003–1-2), hydrogen peroxide (H_2O_2) (A064–1-1), and O^{2-} (A052–1-1) levels were detected using commercial kits (Nanjing Institute of Biotechnology, Nanjing, China).

2.6. Gut microbial community analyses

Microbial genomic DNA, extracted using an E.Z.N.A.® soil DNA kit (Omega Bio-Tek, Norcross, GA, USA), was amplified using V3–V4 *16S rRNA* primers and TransStart FastPfu DNA polymerase. A quantifluorTM-ST Blue quantitative system was used for quantitative analyses. After purification and quantification, PCR products were sequenced on the Illumina MiSeq platform (Shanghai Meiji Biomedical Technology Co., Ltd., Shanghai, China). The average sequencing depth of a single sample was approximately 43,000 reads. Using a sequence similarity of 97%, clean reads were clustered into operational taxonomic units (OTUs) in Usearch (v.7.1). The RDP Bayesian algorithm classifier

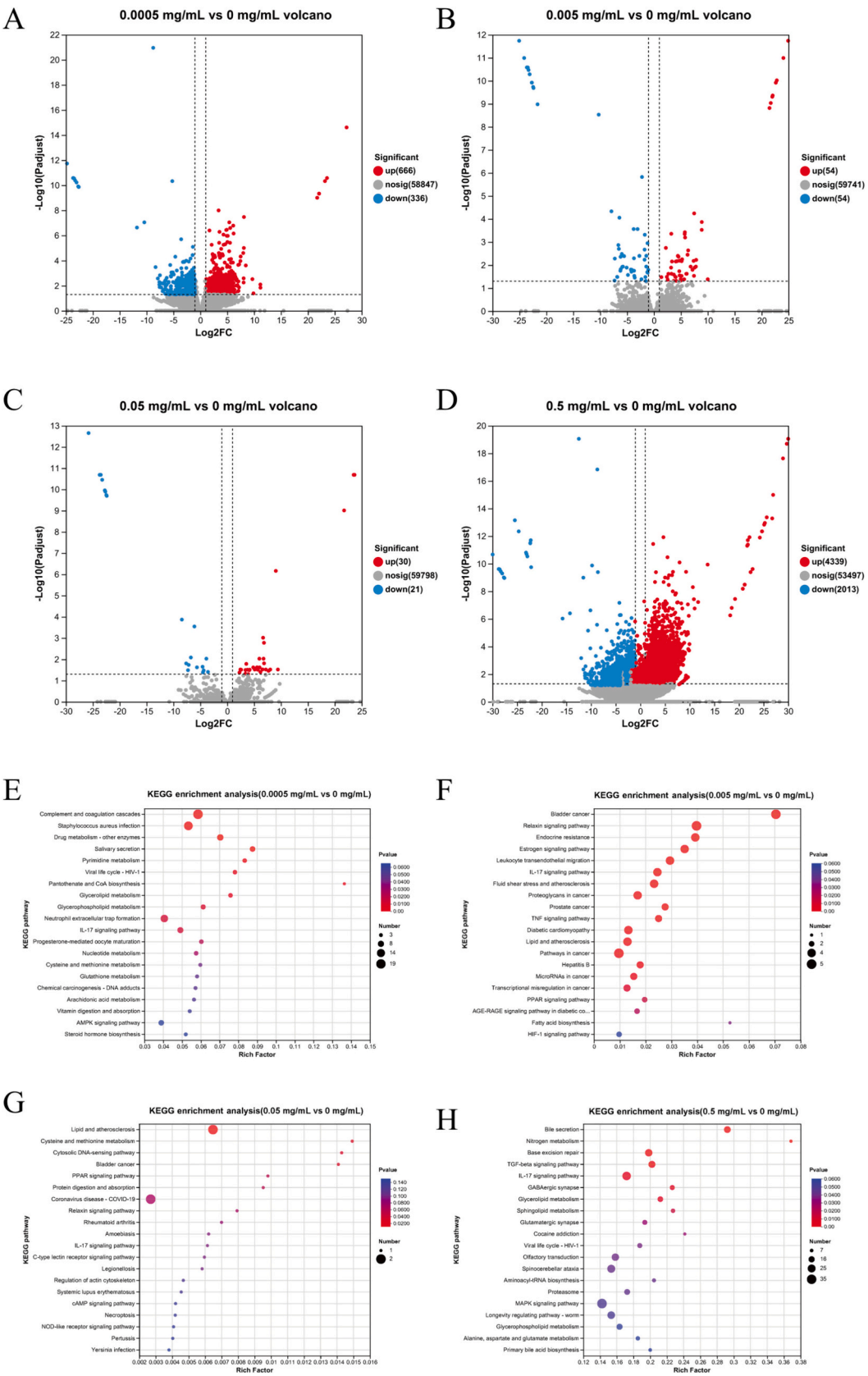

Fig. 4. Transcriptomic analyses of liver samples from black-spotted frogs. Differentially expressed gene (DEG) analyses: Volcano map showing DEGs in (A) 0.0005 mg/mL, (B) 0.005 mg/mL, (C) 0.05 mg/mL, and (D) 0.5 mg/mL TWP leachate groups when compared with controls. Kyoto Encyclopedia of Genes and Genomes enrichment analyses: (E) 0.0005 mg/mL, (F) 0.005 mg/mL, (G) 0.05 mg/mL, and (H) 0.5 mg/mL TWP leachate groups compared with controls.

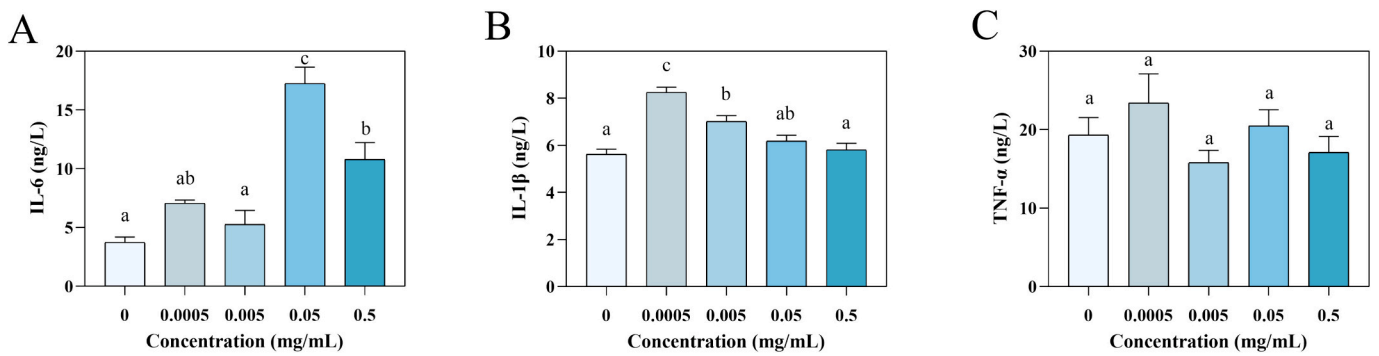

Fig. 5. Pro-inflammatory factor activity levels; IL-6 (A), IL-1β (B), and TNF-α (C) in liver samples (n = 3) from black-spotted frogs exposed to TWP leachates. Different superscripts indicate significant intergroup differences at $p < 0.05$.

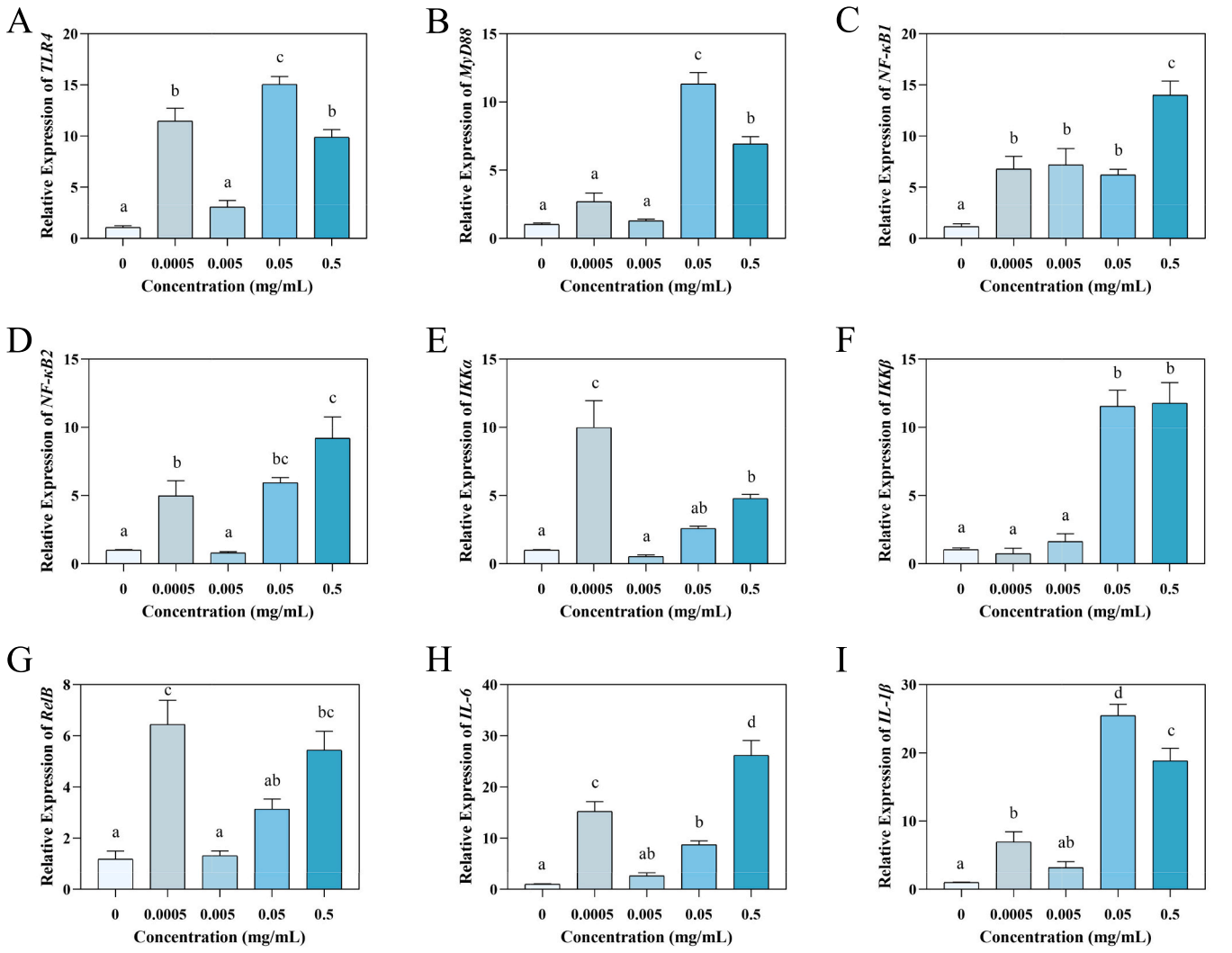

Fig. 6. *TLR4* (A), *MyD88* (B), *NF-κB1* (C), *NF-κB2* (D), *IKKα* (E), *IKKβ* (F), *RelB* (G), *IL-6* (H), and *IL-1β* (I) expression levels in liver samples (n = 3) from black-spotted frogs exposed to TWP leachates. Different superscripts indicate significant intergroup differences at $p < 0.05$.

combined with the Silva database were used to perform a taxonomic analysis of representative sequences with similarity >97% OTUs. Then, community species composition at taxonomic levels was assessed.

2.7. Transcriptome analysis and quantitative real-time PCR (qRT-PCR)

Total RNA was extracted from liver samples using TRIzol (China ComWin Biotechnology Co., Ltd.), after which RNA purity and integrity were examined using a NanoDrop 2000 microphotometer (Thermo Fisher Scientific, USA) and agarose gel electrophoresis.

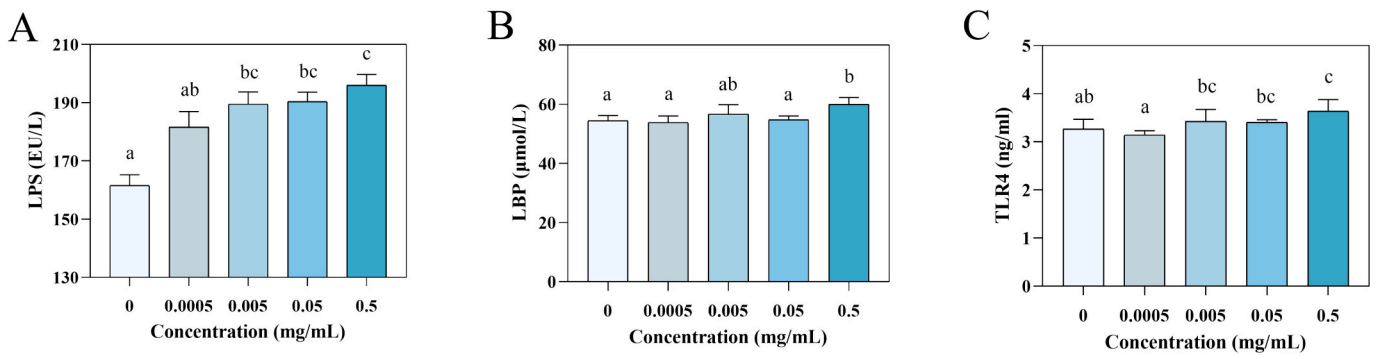

Fig. 7. Lipopolysaccharide content (A) in plasma; lipopolysaccharide-binding protein (B) and toll-like receptor 4 (C) content in liver tissues. Different superscripts indicate significant intergroup differences at $p < 0.05$.

RNA integrity was also assessed using an Agilent 2100 Bioanalyzer. RNA sequencing was performed by Majorbio using the Illumina Novaseq 6000 platform; 2 × 150 bp sequencing was performed by constructing Illumina PE libraries, and read count data analyses performed using the DEseq2 software package to generate fold change values for different genes when compared with controls [22]. Differentially expressed genes (DEGs) were screened using $p < 0.05$ and $|\text{Log2FoldChange}| > 1$ values. DEGs were then used for functional enrichment analyses, including Gene Ontology and Kyoto Encyclopedia of Genes and Genomes (KEGG) assessments. A $p < 0.05$ value was used as the threshold value in enrichment analyses [23].

To verify DEG levels, 15 genes were randomly selected and analyzed using qRT-PCR. Contaminating genomic DNA and RNA reverse transcription procedures were performed using a Hifair® III 1st strand cDNA synthesis SuperMix kit for qPCR (gDNA digester plus) (Yeasen Biotechnology Co., Ltd., China). Primer sequences were designed using the National Center for Biotechnology Information website and synthesized by Sangon Biotechnology Co., Ltd. (Shanghai, China). Then, qRT-PCR was performed using Hieff® qPCR SYBR® Green Master Mix kits (Yeasen Biotechnology Co., Ltd., China) on a CFX 384 Touch RT-PCR detection platform (Bio-Rad, Germany). *GAPDH* was used as an internal control, and the $2^{-\triangle\triangle CT}$ method was used to detect gene transcription levels [36]. All samples had three replicates. Primer sequences are listed (**Table S2**).

2.8. Statistical analysis

Data were analyzed using IBM SPSS statistical software v.20 (IBM, USA) and expressed as the mean ± standard error of the mean. Before parameter tests, Levene's test and Kolmogorov-Smirnov test were used to test normality and homoscedasticity. One-way analysis of variance was used to determine significant differences between experimental groups, then followed by Tukey's post hoc tests. When data distribution was skewed, Kruskal–Wallis tests were performed. A $p < 0.05$ value indicated statistical significance.

3. Results and discussion

3.1. TWP leachate accumulation in frog tissues

As a TWP leachate marker, the trace metal Zn has been identified in exposure solutions [37,38]. In our study, Zn concentrations were below detection limits (0.05 mg/L) in 0.0005, 0.005, and 0.05 mg/mL TWP leachate groups. The Zn concentration in the 0.5 mg/mL group was 0.1573 mg/L before exposure (0 h) and 0.0585 mg/L after 24 h of exposure, a decrease of 62.8% (**Table S1**). This Zn reduction in the exposure solution was presumably absorbed by the black-spotted frog during exposure.

To further confirm that TWP leachates were absorbed by frogs, Zn accumulation in frog tissues, including liver, kidney, spleen, heart, intestine, and gonads, was determined. In general, Zn preferentially accumulated in the intestine, liver, and kidney, while the lowest concentration was observed in the gonad (Fig. 1). With increasing TWP leachate concentrations, Zn accumulation increased in the liver and intestine, indicating that water environments are important Zn absorption sources of TWP leachates by frogs.

3.2. TWP leachate exposure impairs liver function

When compared with controls, hepatosomatic indices from 0.0005, 0.005, 0.05, and 0.5 mg/mL groups trends to be increased the liver coefficient by 1.46-, 1.60-, 1.88-, and 1.56-fold, respectively (Fig. 2A).

Hepatic vacuolization and inflammation are typical liver disease features [39]. After pollutant exposure, amphibian liver tissue pathology is often represented by Kupfer cell hypertrophy, pigmentation, inflammatory cell and liver inflammation, extramedullary hematopoiesis, significant hepatocyte nuclear enlargement, epithelial degeneration, and pulmonary necrosis [40]. In our study, control liver tissues showed normal tissue morphology and typical cell structures and arrangements (Fig. 2B). In contrast, after TWP exposure at various concentrations, inflammatory cell infiltration and diffuse cell boundaries were observed (Fig. 2C–F); when compared with controls, liver inflammatory cell infiltration in the all TWP leachate exposure group was significantly decreased, with aggregated inflammatory cells and significantly increased nuclei (**Fig. 2G**, $p < 0.05$). Additionally, when compared with controls, 0.005, 0.05, and 0.5 mg/mL groups had significantly increased liver vacuolar areas (1.66-, 1.36-, and 1.26-fold, respectively) (**Fig. 2H**, $p < 0.05$). Fig. 2H showed an inverted-U-shaped curves and was consistent with the 'hormesis effect', where low dose of contaminants can promote stimulatory response in organisms, while high concentration elicits inhibitory or toxic effect [41]. Therefore, frog exposure to TWPs at environmentally relevant concentrations appeared to cause liver tissue damage.

3.3. TWP leachate exposure induces hepatic oxidative stress

Generally, ROS production and elimination, including O^{2-} and H_2O_2, occur in equilibrium in organisms [42]. However, when aquatic organisms are exposed to environmental contaminants, this dynamic equilibrium is disrupted, resulting in elevated ROS levels [42]. In our study, 0.05 mg/mL TWP leachate exposure significantly increased hepatic O^{2-} activity when compared with controls ($p < 0.05$; Fig. 3A). The 0.0005, 0.05, and 0.5 mg/mL exposure groups showed significantly increased hepatic H_2O_2 content ($p < 0.05$; Fig. 3B). Therefore, TWP leachates appeared to increase ROS content.

Enzyme activity levels related to antioxidant defenses were also investigated. When TWP leachate concentrations increased, SOD and GST enzyme activities increased significantly (**Fig. 3C, E**, $p < 0.05$).

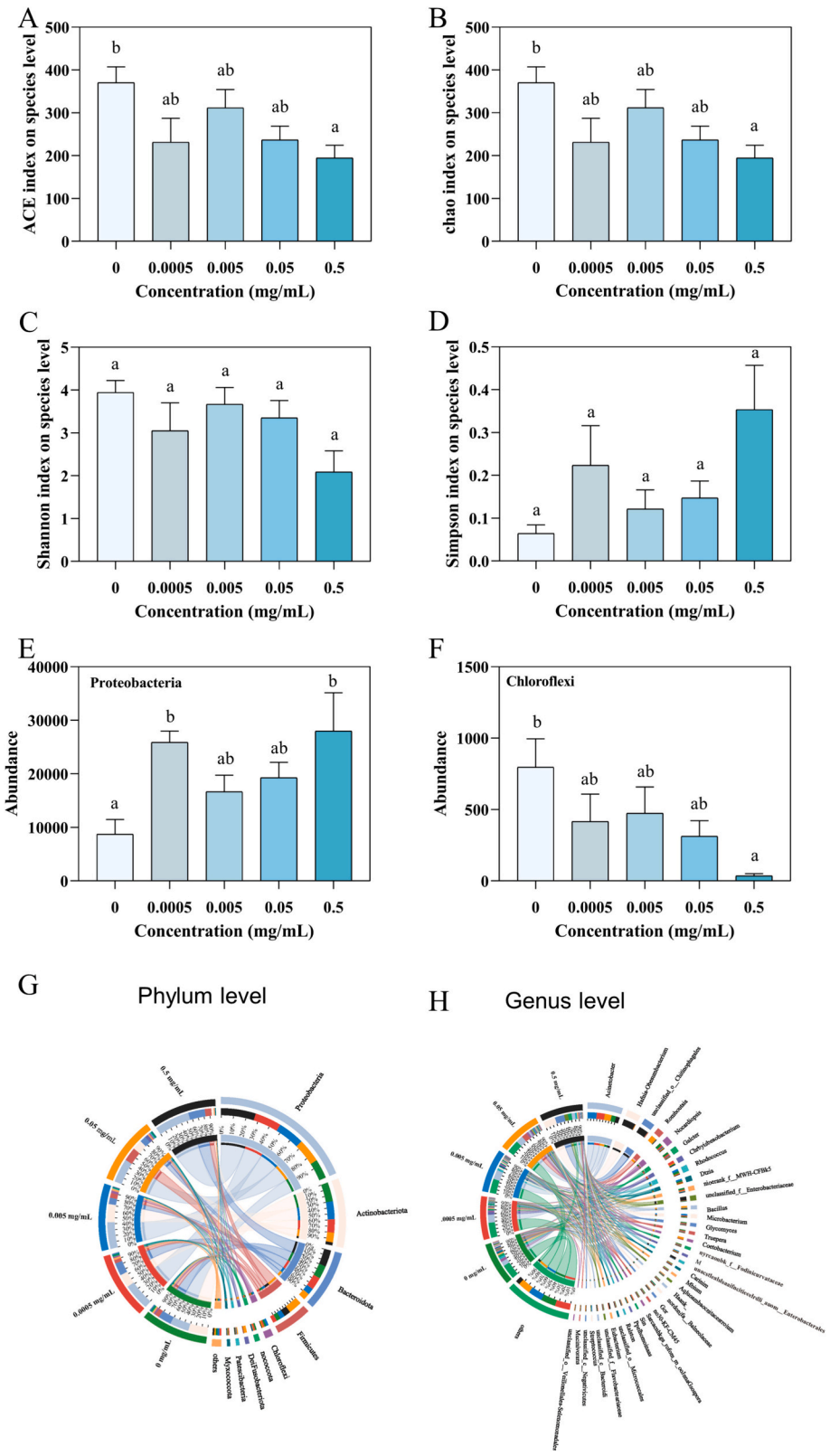

Fig. 8. Gut microbiome α-diversity analyses; (A) ACE, (B) Chao, (C) Shannon, and (D) Simpson indices ($n = 6$). *Proteobacteria* (E) and *Choroflexi* abundance (F); Intestinal sample distribution across different groups at phylum (G) and genus levels (H). Different superscripts indicate significant intergroup differences at $p < 0.05$.

However, no significant changes in GPX levels were observed in livers exposed to TWP leachates (Fig. 3**D**, $p > 0.05$). Importantly, SOD enzyme activity showed a dramatic impact, and was possibly related to specific functions; SOD converts superoxide to H_2O_2, which is further detoxified to water or other harmless substance by GST and GPX [43]. Thus, SOD activity may function as a suitable environmental contaminant biomarker, especially for TWP leachates [44,45]. Therefore, ROS levels in black-spotted frog livers showed overall upward trends after TWP

leachate exposure, with antioxidant enzyme activity similarly increased. These observations suggested that TWP leachate exposure induced hepatic oxidative stress in frogs.

3.4. Liver transcriptomics show inflammation effects

To further determine liver injury mechanisms induced by TWP leachate exposure, we conducted a global transcriptomics analysis of controls and TWP leachate-exposed frogs. In total, 1002 (666 downregulated and 336 upregulated), 108 (54 downregulated and 54 upregulated), 51 (30 downregulated and 21 upregulated), and 6352 (4339 downregulated and 2013 upregulated) DEGs were identified in 0.0005, 0.005, 0.05, and 0.5 mg/mL groups, respectively (Fig. 4A–D). To further explore DEG biological functions, KEGG pathway enrichment analyses showed that all TWP leachate concentrations enriched IL-17 signaling, which is implicated in inflammation (Fig. 4E–H). Also, inflammation-related signaling pathways such as TNF and tumor growth factor-β pathways were significantly enriched in 0.005 and 0.5 mg/mL groups ($p < 0.05$), indicating that TWP mainly interfered with liver inflammation processes in these frogs.

IL-1β, IL-6, and TNF-α are typical pro-inflammatory cytokines that inhibit and eliminate inflammation by activating local and systemic inflammatory responses [46,47]. When compared with controls, liver IL-6 levels were significantly increased in frogs exposed to 0.05 and 0.5 mg/mL TWP leachates and IL-β activity were increased in 0.0005 and 0.005 mg/mL ($p < 0.05$; Fig. 5A, B). While, no significant difference was observed in the TNF-α after exposure to TWP leachates, which suggested that TNF-α was not a suitable biomarker of TWP. Thus, upregulated IL-1β and IL-6 levels indicated inflammatory responses in liver tissues, consistent with transcriptomic data.

3.5. TWP leachates induce toll-like receptor 4 (TLR4)-nuclear factor (NF)-κB signaling

Liver inflammation may be enhanced by TLR4 and NF-κB [48]. Thus, to further confirm our transcriptomic data, TLR4-NF-κB signaling levels were determined. After a 21 day TWP leachate exposure, significantly higher *TLR4*, *MyD88*, *NF-κB1*, *NF-κB2*, *IKKα,* and *IKKβ* expression levels were observed in frog livers (**Fig. 6A–F**, $p < 0.05$), except in the 0.005 mg/mL exposure group. Specifically, related pathway gene expression (*NF-κB1*, *NF-κB2*, *IKKα,* and *IKKβ*) was increased, but varied at different leachate concentrations. In general, all genes were significantly increased in the 0.5 mg/mL group. *NF-κB1*, *NF-κB2*, and *IKKα* were statistically significant increased after exposure to 0.0005 mg/mL. No statistical differences in *NF-κB2*, *IKKα,* and *IKKβ* expression were observed after 0.005 mg/mL exposure ($p > 0.05$; Fig. 6D, E). Therefore, TWP leachate exposure may have activated TLR4-NF-κB signaling in black-spotted frog livers.

3.6. TWP leachate exposure causes intestinal microbiome dysbiosis

TLR4 activation in the liver is related to LPS-binding protein (LBP) content in the liver and LPS content in plasma [36]. LPS content increased significantly in the 0.005, 0.05, and 0.5 mg/mL TWP leachate group, and showed dose-dependent increases with TWP exposure concentrations (Fig. 7A; $p < 0.05$). Also, LBP and TLR4 content in liver tissues increased significantly in the 0.5 mg/mL group (Fig. 7B, C; $p < 0.05$).

As a bacterial endotoxin, LPS is a major biomarker of microbiome dysbiosis [49]. In our study, no significant differences ($p > 0.05$) between ACE, Chao, and Shannon indices in 0.0005 mg/mL and 0.005 mg/mL groups were observed when compared with controls (Fig. 8A-C), while the Simpson index was trend to be increased (**Fig. 8D,** $p > 0.05$). ACE and Chao in the 0.5 mg/mL TWP leachate group were significantly reduced (**Fig. 8A–C**, $p < 0.05$), while the Simpson index was trend to be increased ($p > 0.05$). These observations indicated that TWP leachate exposure inhibited intestinal flora richness in black-spotted frogs, but significantly increased diversity.

TWP leachate exposure altered bacterial abundance at both phylum and family levels; *Chloroflexi* abundance was significantly decreased but *Proteobacteria* abundance was significantly increased in the 0.5 mg/mL TWP leachate exposure group (**Fig. 8E-H**, $p < 0.05$). *Proteobacteria* is a major source of gut–derived endotoxic LPS, and its abundance is associated with intestinal LPS levels [50]. In our study, *Proteobacteria* proportions drastically increased by up to 2.97-, 1.91-, 2.21-, and 3.21-fold after 0.0005, 0.005, 0.05, and 0.5 mg/mL TWP leachate exposure, respectively, which were likely associated with increased fecal LPS concentrations. Such elevated plasma LPS levels may be attributed to TWP-induced gut microbiota dysbiosis, e.g., increased *Proteobacteria* abundance [51,52]. Similarly, a disordered intestinal flora will exhibit correlations with inflammatory factors and antioxidant and oxidation products in the liver.

The gut and liver are tightly linked and communicate via the portal vein and biliary system, with the liver constantly exposed to gut-derived bacterial products and metabolites, e.g., LPS [53]. Intestinal-derived LPS is sensed by TLRs expressed on hepatic macrophages, with the LPS–TLR axis (especially TLR4) inducing hepatic macrophage hyperactivation [20]. Mechanistically, LPS activates hepatic macrophages by binding to TLR4 and activating NF-κB, thereby activating these cells to secrete IL-1β and IL-6, lysosomal enzymes (proteases and phosphatases), and superoxides, thus aggravating inflammation. Therefore, LPS gut-derived effects on liver injury may depend on exposure time and duration [54].

TWP leachates at realistic environmental levels may cause intestinal microbiome dysbiosis. This may elevate LPS levels in plasma, which activate downstream immune pathways (TLR4/NF-κB) by binding to LBP and triggering inflammation reactions (elevated IL-1β and IL-6) and oxidative damage (elevated ROS) and other damage (elevated histopathology) in the liver. As TWP leachates was a mixture, further research is required to identify the main toxigenic components in these leachates [55].

CRediT authorship contribution statement

Zhiquan Liu: Writing – review & editing, Writing – original draft, Funding acquisition, Conceptualization. **Hongmei Yang:** Writing – review & editing, Writing – original draft, Visualization. **Yinan Zhang:** Writing – review & editing, Writing – original draft, Visualization. **Yongjian Shao:** Writing – review & editing, Writing – original draft, Visualization. **Shuangqing Hu:** Writing – review & editing, Writing – original draft, Visualization. **Hangjun Zhang:** Writing – review & editing, Writing – original draft, Visualization. **Genxiang Shen:** Writing – review & editing, Supervision, Resources, Project administration.

Declaration of competing interest

The authors declare that they have no known competing financial interests or personal relationships that could have appeared to influence the work reported in this paper.

Acknowledgments

This study was funded by the State Environmental Protection Key Laboratory of Environmental Health Impact Assessment of Emerging Contaminants (SEPKL-EHIAEC-202201), Natural Science Foundation of Zhejiang Province of China (LQ22C030003), the National Natural Science Foundation of China (42207323), “Pioneer” and “Leading Goose” R and D Program of Zhejiang (2023C03130).

Appendix A. Supplementary data

Supplementary data to this article can be found online at https://doi.org/10.1016/j.enceco.2024.08.004.

References

[1] P.J. Kole, A.J. Löhr, F.G. Van Belleghem, A.M. Ragas, Wear and tear of tyres: a stealthy source of microplastics in the environment, Int. J. Environ. Res. Public Health 14 (2017) 1265.

[2] N.B. Hartmann, T. Hüffer, R.C. Thompson, M. Hassellöv, A. Verschoor, A. E. Daugaard, S. Rist, T. Karlsson, N. Brennholt, M. Cole, M.P. Herrling, M.C. Hess, N.P. Ivleva, A.L. Lusher, M. Wagner, Response to the letter to the editor regarding our feature "are we speaking the same language? Recommendations for a definition and categorization framework for plastic debris", Environ. Sci. Technol. 53 (2019) 4678–4679.

[3] A. Das, S.K. Ray, M. Mohanty, J. Mohanty, S. Dey, A.P. Das, Ecotoxicity of microplastic wastes and their sustainable management: a review, Environ. Chem. Ecotoxicol. 6 (2024) 144–152.

[4] A.M. O'Brien, T.F. Lins, Y. Yang, M.E. Frederickson, D. Sinton, C.M. Rochman, Microplastics shift impacts of climate change on a plant-microbe mutualism: temperature, CO_2, and tire wear particles, Environ. Res. 203 (2022) 111727.

[5] M. Siegfried, A.A. Koelmans, E. Besseling, C. Kroeze, Export of microplastics from land to sea. A modelling approach, Water Res. 127 (2017) 249–257.

[6] P.E. Redondo-Hasselerharm, V.N. de Ruijter, S.M. Mintenig, A. Verschoor, A. A. Koelmans, Ingestion and chronic effects of car tire tread particles on freshwater benthic macroinvertebrates, Environ. Sci. Technol. 52 (2018) 13986–13994.

[7] A. Wik, J. Lycken, G. Dave, Sediment quality assessment of road runoff detention systems in Sweden and the potential contribution of tire wear, Water Air Soil Pollut. 194 (2008) 301–314.

[8] A. Wik, G. Dave, Occurrence and effects of tire wear particles in the environment - a critical review and an initial risk assessment, Environ. Pollut. 157 (2009) 1–11.

[9] J.K. McIntyre, J. Prat, J. Cameron, J. Wetzel, E. Mudrock, K.T. Peter, Z.Y. Tian, C. Mackenzie, J. Lundin, J.D. Stark, K. King, J.W. Davis, E.P. Kolodziej, N.L. Scholz, Treading water: tire wear particle leachate recreates an urban runoff mortality syndrome in Coho but not chum Salmon, Environ. Sci. Technol. 55 (2021) 11767–11774.

[10] L. Zimmermann, G. Dierkes, T.A. Ternes, C. Völker, M. Wagner, Benchmarking the in vitro toxicity and chemical composition of plastic consumer products, Environ. Sci. Technol. 53 (2019) 11467–11477.

[11] Z.-M. Li, K. Kannan, Occurrence of 1,3-diphenylguanidine, 1,3-Di-o-tolylguanidine, and 1,2,3-triphenylguanidine in indoor dust from 11 countries: implications for human exposure, Environ. Sci. Technol. 57 (2023) 6129–6138.

[12] Z.-M. Li, V.K. Pal, P. Kannan, W. Li, K. Kannan, 1,3-Diphenylguanidine, benzothiazole, benzotriazole, and their derivatives in soils collected from northeastern United States, Sci. Total Environ. 887 (2023) 164110.

[13] J.-R. Jiang, Z.-F. Chen, X.-L. Liao, Q.-Y. Liu, J.-M. Zhou, S.-P. Ou, Z. Cai, Identifying potential toxic organic substances in leachates from tire wear particles and their mechanisms of toxicity to Scenedesmus obliquus, J. Hazard. Mater. 458 (2023) 132022.

[14] X. Ni, H. Zhou, Y. Liu, J. Zhan, Q. Meng, H. Song, X. Yi, Toxic effects of tire wear particles and the leachate on the Chinese mitten crab (Eriocheir sinensis), Environ. Pollut. 335 (2023) 122354.

[15] L.L. Halle, A. Palmqvist, K. Kampmann, A. Jensen, T. Hansen, F.R. Khan, Tire wear particle and leachate exposures from a pristine and road-worn tire to Hyalella azteca: comparison of chemical content and biological effects, Aquat. Toxicol. 232 (2021) 105769.

[16] T. Zhao, Y. Zhang, Q. Song, Q. Meng, S. Zhou, J. Cong, Tire and road wear particles in the aquatic organisms – a review of source, properties, exposure routes, and biological effects, Aquat. Toxicol. 273 (2024) 107010.

[17] P.P. Song, N. Jiang, K.Q. Zhang, X.X. Li, N. Li, Y.A. Zhang, Q. Wang, J. Wang, Ecotoxicological evaluation of zebrafish liver (Danio rerio) induced by dibutyl phthalate, J. Hazard. Mater. 425 (2022).

[18] P.D. Ray, B.W. Huang, Y. Tsuji, Reactive oxygen species (ROS) homeostasis and redox regulation in cellular signaling, Cell. Signal. 24 (2012) 981–990.

[19] Y.F. Sheng, Y. Liu, K.W. Wang, J.V. Cizdziel, Y.C. Wu, Y. Zhou, Ecotoxicological effects of micronized car tire wear particles and their heavy metals on the earthworm (Eisenia fetida) in soil, Sci. Total Environ. 793 (2021).

[20] D. Tian, Y. Yu, Y. Yu, L. Lu, D. Tong, W. Zhang, X. Zhang, W. Shi, G. Liu, Tris (2-chloroethyl) phosphate exerts hepatotoxic impacts on zebrafish by disrupting hypothalamic–pituitary–thyroid and gut–liver axes, Environ. Sci. Technol. 57 (2023) 9043–9054.

[21] J. Wen, H. Sun, B. Yang, E. Song, Y. Song, G. Jiang, Environmentally relevant concentrations of microplastic exposure cause cholestasis and bile acid metabolism dysregulation through a gut-liver loop in mice, Environ. Sci. Technol. 58 (2024) 1832–1841.

[22] T. Ku, Y. Liu, Y. Xie, J. Hu, Y. Hou, X. Tan, X. Ning, G. Li, N. Sang, Tebuconazole mediates cognitive impairment via the microbe-gut-brain axis (MGBA) in mice, Environ. Int. 173 (2023) 107821.

[23] B. Han, J. Li, S. Li, Y. Liu, Z. Zhang, Effects of thiacloprid exposure on microbiota–gut–liver axis: multiomics mechanistic analysis in Japanese quails, J. Hazard. Mater. 442 (2023) 130082.

[24] C. Thapliyal, A. Priya, S.B. Singh, V. Bahuguna, A. Daverey, Potential strategies for bioremediation of microplastic contaminated soil, Environ. Chem. Ecotoxicol. 6 (2024) 117–131.

[25] H. Zhang, J. Wu, N. Fang, S. Zhang, X. Su, H. Jiang, P. Hong, H. Wu, Y. Shu, Waterborne exposure to microcystin-leucine arginine induces endocrine disruption and gonadal dysplasia of Pelophylax nigromaculatus tadpoles via the hypothalamic-pituitary-gonadal-liver axis, Sci. Total Environ. 906 (2024) 167644.

[26] E.F. Zipkin, G.V. DiRenzo, J.M. Ray, S. Rossman, K.R. Lips, Tropical snake diversity collapses after widespread amphibian loss, Science 367 (2020) 814–816.

[27] S.J. O'hanlon, A. Rieux, R.A. Farrer, G.M. Rosa, B. Waldman, A. Bataille, T. A. Kosch, K.A. Murray, B. Brankovics, M. Fumagalli, Recent Asian origin of chytrid fungi causing global amphibian declines, Science 360 (2018) 621–627.

[28] V.K. Llewelyn, L. Berger, B.D. Glass, Percutaneous absorption between frog species: variability in skin may influence delivery of therapeutics, J. Vet. Pharmacol. Ther. 43 (2020) 91–95.

[29] Z. Liu, Y. Zhang, X. Jia, T.D. Hoskins, L. Lu, Y. Han, X. Zhang, H. Lin, L. Shen, Y. Feng, Y. Zheng, C. Hu, H. Zhang, Microcystin-LR induces estrogenic effects at environmentally relevant concentration in black-spotted pond frogs (*Pelophylax nigromaculatus*): In situ, in vivo, in vitro, and in silico investigations, Environ. Sci. Technol. 58 (2024) 9559–9569.

[30] X. Du, B. Yuan, Y. Zhou, Z. Zheng, Y. Wu, Y. Qiu, J. Zhao, G. Yin, Tissue-specific accumulation, sexual difference, and maternal transfer of chlorinated Paraffins in black-spotted frogs, Environ. Sci. Technol. 53 (2019) 4739–4746.

[31] H. Lin, Z. Liu, H. Yang, L. Lu, R. Chen, X. Zhang, Y. Zhong, H. Zhang, Per- and polyfluoroalkyl substances (PFASs) impair lipid metabolism in *Rana nigromaculata*: a field investigation and laboratory study, Environ. Sci. Technol. 56 (2022) 13222–13232.

[32] Z. Liu, C. Shi, B. Wang, X. Zhang, J. Ding, P. Gao, X. Yuan, Z. Liu, H. Zhang, Cytochrome P450 enzymes in the black-spotted frog (Pelophylax nigromaculatus): molecular characterization and upregulation of expression by sulfamethoxazole, Front. Physiol. 15 (2024) 1412943.

[33] E.G. Xu, N. Lin, R.S. Cheong, C. Ridsdale, R. Tahara, T.Y. Du, D. Das, J. Zhu, L. Peña Silva, A. Azimzada, H.C.E. Larsson, N. Tufenkji, Artificial turf infill associated with systematic toxicity in an amniote vertebrate, Proc. Natl. Acad. Sci. 116 (2019) 25156–25161.

[34] J.E. Tamis, A.A. Koelmans, R. Dröge, N.H.B.M. Kaag, M.C. Keur, P.C. Tromp, R. H. Jongbloed, Environmental risks of car tire microplastic particles and other road runoff pollutants, Microplast. Nanoplast. 1 (2021) 10.

[35] B. Hou, F. Wang, T. Liu, Z. Wang, Reproductive toxicity of polystyrene microplastics: in vivo experimental study on testicular toxicity in mice, J. Hazard. Mater. 405 (2021) 124028.

[36] K.J. Livak, T.D. Schmittgen, Analysis of relative gene expression data using real-time quantitative PCR and the $2-\Delta\Delta CT$ method, Methods 25 (2001) 402–408.

[37] T. Masset, B.J.D. Ferrari, D. Oldham, W. Dudefoi, M. Minghetti, K. Schirmer, A. Bergmann, E. Vermeirssen, F. Breider, In vitro digestion of Tire particles in a fish model (Oncorhynchus mykiss): solubilization kinetics of heavy metals and effects of food coingestion, Environ. Sci. Technol. 55 (2021) 15788–15796.

[38] P. Klöckner, T. Reemtsma, P. Eisentraut, U. Braun, A.S. Ruhl, S. Wagner, Tire and road wear particles in road environment–quantification and assessment of particle dynamics by Zn determination after density separation, Chemosphere 222 (2019) 714–721.

[39] T. Lu, J. Liu, E.L. LeCluyse, Y.S. Zhou, M.L. Cheng, M.P. Waalkes, Application of cDNA microarray to the study of arsenic-induced liver diseases in the population of Guizhou, China, Toxicol. Sci. Off. J. Soc. Toxicol. 59 (2001) 185–192.

[40] U.A. Jayawardena, P. Angunawela, D.D. Wickramasinghe, W.D. Ratnasooriya, P. V. Udagama, Heavy metal-induced toxicity in the Indian Green frog: biochemical and histopathological alterations, Environ. Toxicol. Chem. 36 (2017) 2855–2867.

[41] M.P. Mattson, Hormesis defined, Ageing Res. Rev. 7 (2008) 1–7.

[42] C.-B. Jeong, E.-J. Won, H.-M. Kang, M.-C. Lee, D.-S. Hwang, U.-K. Hwang, B. Zhou, S. Souissi, S.-J. Lee, J.-S. Lee, Microplastic size-dependent toxicity, oxidative stress induction, and p-JNK and p-p38 activation in the monogonont rotifer (Brachionus koreanus), Environ. Sci. Technol. 50 (2016) 8849–8857.

[43] C. Shi, Z. Liu, B. Yu, Y. Zhang, H. Yang, Y. Han, B. Wang, Z. Liu, H. Zhang, Emergence of nanoplastics in the aquatic environment and possible impacts on aquatic organisms, Sci. Total Environ. 167404 (2023).

[44] Y.G. Niu, X.J. Zhang, H.Y. Zhang, T.S. Xu, S.K. Men, K.B. Storey, Q. Chen, Antioxidant and non-specific immune defenses in partially freeze-tolerant Xizang plateau frogs, Nanorana parkeri, J. Therm. Biol. 102 (2021).

[45] S. Dahms-Verster, A. Nel, J.H.J. van Vuren, R. Greenfield, Biochemical responses revealed in an amphibian species after exposure to a forgotten contaminant: An integrated biomarker assessment, Environ. Toxicol. Pharmacol. 73 (2020).

[46] D.L. Feng, R.Y. Guo, W. Liao, J.C. Li, S. Cao, Plantamajoside alleviates acute sepsis-induced organ dysfunction through inhibiting the TRAF6/NF-κB axis, Pharm. Biol. 61 (2023) 897–906.

[47] X.Y. Fang, J.M. Cao, Z. Tao, Z.Q. Yang, Y. Dai, L.G. Zhao, Hydroxytyrosol attenuates ethanol-induced liver injury by ameliorating steatosis, oxidative stress and hepatic inflammation by interfering STAT3/iNOS pathway, Redox Rep. 28 (2023).

[48] S.-N. Chen, Y. Tan, X.-C. Xiao, Q. Li, Q. Wu, Y.-Y. Peng, J. Ren, M.-L. Dong, Deletion of TLR4 attenuates lipopolysaccharide-induced acute liver injury by inhibiting inflammation and apoptosis, Acta Pharmacol. Sin. 42 (2021) 1610–1619.

[49] B.R. Stevens, R. Goel, K. Seungbum, E.M. Richards, R.C. Holbert, C.J. Pepine, M. K. Raizada, Increased human intestinal barrier permeability plasma biomarkers zonulin and FABP2 correlated with plasma LPS and altered gut microbiome in anxiety or depression, Gut 67 (2018) 1555–1557.

[50] P. Zhang, L. Zheng, Y. Duan, Y. Gao, H. Gao, D. Mao, Y. Luo, Gut microbiota exaggerates triclosan-induced liver injury via gut-liver axis, J. Hazard. Mater. 421 (2022) 126707.

[51] B. Huang, M.X. Gui, H.L. An, J.Y. Shen, F.M. Ye, Z.A. Ni, H.Z. Zhan, L. Che, Z.C. Lai, J.H. Zeng, J. Peng, J.M. Lin, Babao Dan alleviates gut immune and microbiota disorders while impacting the TLR4/MyD88/NF-?B pathway to attenuate 5-fluorouracil-induced intestinal injury, Biomed. Pharmacother. 166 (2023).

[52] W.S. Zhou, W. Shi, X.Y. Du, Y. Han, Y. Tang, S. Ri, K. Ju, T. Kim, L. Huang, W. X. Zhang, Y.H. Yu, D.D. Tian, Y.Y. Yu, L.B. Chen, Z.C. Wu, G.X. Liu, Assessment of nonalcoholic fatty liver disease symptoms and gut-liver axis status in zebrafish after exposure to polystyrene microplastics and oxytetracycline, alone and in combination, Environ. Health Perspect. 131 (2023).

[53] X. Fang, J. Cao, Z. Tao, Z. Yang, Y. Dai, L. Zhao, Hydroxytyrosol attenuates ethanol-induced liver injury by ameliorating steatosis, oxidative stress and hepatic inflammation by interfering STAT3/iNOS pathway, Redox Rep. 28 (2023) 2187564.

[54] A. Wahlström, Outside the liver box: The gut microbiota as pivotal modulator of liver diseases, Biochim. Biophys. Acta (BBA)-Mol. Basis Dis. 1865 (2019) 912–919.

[55] Z. Tian, H. Zhao, K.T. Peter, M. Gonzalez, J. Wetzel, C. Wu, X. Hu, J. Prat, E. Mudrock, R. Hettinger, A.E. Cortina, R.G. Biswas, F.V.C. Kock, R. Soong, A. Jenne, B. Du, F. Hou, H. He, R. Lundeen, A. Gilbreath, R. Sutton, N.L. Scholz, J. W. Davis, M.C. Dodd, A. Simpson, J.K. McIntyre, E.P. Kolodziej, A ubiquitous tire rubber–derived chemical induces acute mortality in coho salmon, Science 371 (2021) 185–189.